(28) Yamazaki, I.; Kume, H.; Tamai, N.; Tsuchiya, H.; Oba, K. *Rev. Sci. Instrum.* **1985**, *56*, 1187.
(29) (a) Kanaya, T.; Hatano, Y.; Yamamoto, M.; Nishijima, Y. *Bull. Chem. Soc. Jpn.* **1979**, *52*, 2079. (b) Ito, S.; Yamamoto, M.; Nishijima, Y. *Bull. Chem. Soc. Jpn.* **1982**, *55*, 363.
(30) Ikeda, T.; Lee, B.; Kurihara, S.; Tazuke, S.; Ito, S.; Yamamoto, M. *J. Am. Chem. Soc.* **1988**, *110*, 8299.
(31) (a) Brant, D. A.; Flory, P. J. *J. Am. Chem. Soc.* **1965**, *87*, 2791. (b) Abe, A.; Jernigan, R. L.; Flory, P. J. *J. Am. Chem. Soc.* **1966**, *88*, 631. (c) Yoon, D. Y.; Sundararajan, P. R.; Flory, P. J. *Macromolecules* **1975**, *8*, 776.
(32) Wesson, L. G. *Tables of Electric Dipole Moments*; Technology: Cambridge, 1948.
(33) Szwarc, M. *Carbanions, Living Polymers, and Electron-Transfer Processes*; Interscience: New York, 1968.
(34) Kurahashi, M.; Fukuyo, M.; Shimada, A. *Bull. Chem. Soc. Jpn.* **1969**, *42*, 2174.
(35) Popova, E. G.; Chetkina, L. A. *J. Struct. Chem.* **1979**, *20*, 564.
(36) Sundararajan, P. R. *Macromolecules* **1980**, *13*, 512.
(37) Birks, J. B. *Photophysics of Aromatic Molecules*; Wiley: London, 1970.
(38) Bovey, F. A. *High Resolution NMR of Macromolecules*; Academic: New York, 1972.
(39) Abe, A.; Kobayashi, H.; Kawamura, T.; Date, M.; Uryu, T.; Matsuzaki, K. *Macromolecules* **1988**, *21*, 3414.

Registry No. BCz, 37500-95-1; BEtCz, 51545-40-5; *meso*-BCzPe, 126457-39-4; (±)-BCzPe, 126424-15-5; PBVCz, 120468-30-6; BVCz, 120468-29-3; *tert*-butyl chloride, 507-20-0; bromoethane, 74-96-4; 2,4-bis(tosyloxy)pentane, 35196-66-8; 9-(2-chloroethyl)-3,6-di-*tert*-butylcarbazole, 120484-95-9; carbazole, 86-74-8.

Fluorescence Studies of Coalescence and Film Formation in Poly(methyl methacrylate) Nonaqueous Dispersion Particles[1]

Önder Pekcan[2] and Mitchell A. Winnik*

Department of Chemistry and Erindale College, University of Toronto, Toronto, Ontario, Canada M5S 1A1

Melvin D. Croucher

Xerox Research Centre of Canada, 2660 Speakman Drive, Mississauga, Ontario, Canada L5K 2L1

Received August 3, 1989; Revised Manuscript Received November 15, 1989

ABSTRACT: Poly(methyl methacrylate) [PMMA] particles (d = 1 μm) were prepared by nonaqueous dispersion polymerization. One batch of particles was labeled with phenanthrene [Phe] groups, and a second batch, with anthracene [An]. When mixed, spread as thin films, and then heated above the glass transition temperature of the PMMA, coalescence occurred. Particle fusion was accompanied by increasing amounts of nonradiative energy from Phe* to An. Energy transfer was followed quantitatively by carrying out fluorescence decay measurements on samples quenched to room temperature. The data fit nicely to a Fickian diffusion model and yield values of the diffusion coefficients, D, on the order of 10^{-15} cm^2 s^{-1}. These D values characterize the diffusion of (labeled) polymer molecules across the particle–particle boundary. Since the PMMA in the particles has a broad molecular weight distribution, the D values represent an ensemble average over that distribution.

When dispersions of latex particles are allowed to dry, coalescence occurs to form a continuous polymer film if drying occurs above a certain minimum temperature, called, appropriately, the minimum film-forming temperature [MFT].[3] Coalescence is the essential step in all coating applications of latex-based preparations, and the topic has received extensive attention, particularly by the paint industry. Some traditional concerns have been, for example, the dependence of the MFT on particle composition, size, and morphology.[4,5] Also very important in the case of aqueous latex preparations is an understanding of the forces generated, and their origin, during water evaporation from the coating.[6] These forces must be sufficiently strong to induce deformations in the particle from their original spherical shape to close-packed polyhedra and then to promote fusion into continuous films.

While the issue of molecular diffusion of polymer molecules during coalescence has always been recognized, it is only recently that tools have become available to study this process directly. The fundamental question is, first, to what extent polymer molecules diffuse across the particle boundary during film formation, and, second, how this diffusion depends upon latex composition and structure.

There have been a number of indirect approaches to this question. In transmission electron microscopy [TEM], one can often see the particle boundaries in newly formed films. These have a characteristic hexagonal shape.[7] Since the surface of many latex particles is negatively charged, the interparticle interfaces in the film can be stained for TEM measurements. One curious feature to emerge from the TEM studies is that, in some instances, the particle boundaries eventually disappear,[8] suggesting extensive polymer diffusion across the interface, while in other cases, these particle boundaries persist for weeks and months.[7]

Another approach to the question of latex fusion involves measuring the permeability of the latex films to gasses and vapors. Solvent-cast films are normally continuous and provide a benchmark against which latex films can be compared. Chainey et al.[9] have studied the time evolution of the permeability of latex films. They found that this permeability decreased substantially with time but never reached the same low level obtained in films of the same material prepared by solvent casting. These results were interpreted by assuming that, in the latex

0024-9297/90/2223-2673$02.50/0

films, *polymer segments* diffused across the interface but that sufficient vestiges of the particle boundaries remained for vapors to permeate through these interstitial spaces.

There are two obvious modern techniques which one could use to study diffusion of polymer molecules across the particle boundary. The first involves small-angle neutron scattering [SANS] using deuterium-labeled latex particles. Pioneering steps in this direction were taken by Hahn[10] and more recently by Sperling.[11] Hahn et al. prepared small (80 nm) latex particles from deuterated butyl methacrylate and mixed these with an excess of similar perprotiopoly(butyl methacrylate) particles. Films were formed, and the SANS technique was used to measure the rms radius of gyration (R_G) of the deuterated particles. Polymer diffusion occurred within the films, leading to an increase of R_G with time and a decrease in overall signal strength as the perprotio and perdeuterio polymers interdiffused.

The second technique that should lend itself to studying polymer diffusion during latex film formation involves direct nonradiative energy transfer [DET][12] measurements on films formed from particles suitably labeled with fluorescent dyes. There are various ways in which such experiments might be carried out. One could draw on the wealth of examples published by Morawetz and his group[13] in which DET experiments were used to study mixing in polymer blends as well as polymer diffusion. Their reliance on steady-state fluorescence measurements to determine the efficiency of energy transfer is useful only for very thin films. For films as thick as 50 μm, reabsorption of emitted light becomes problematic. We were interested in developing a new method for studying polymer mixing which avoids altogether the problem of radiative energy transfer. This paper presents our initial results.

For these initial experiments we chose not to prepare simple model aqueous latex particles. Such materials will be examined in future work. We had in hand poly(methyl methacrylate) [PMMA] particles prepared by nonaqueous dispersion [NAD] polymerization.[14] These particles were labeled with appropriate donor [phenanthrene, Phe] and acceptor [anthracene, Phe] and acceptor [anthracene, An] chromophores[15] and were thoroughly characterized.[15-17] They allowed us to proceed directly with our major objective: to test the usefulness of fluorescence decay analysis of DET experiments to follow polymer diffusion during film formation.

The 1-μm-diameter particles we examine have two components. The major component, PMMA, comprises 96 mol % monomer of the material. The minor component, polyisobutylene [PIB, 4 mol % monomer], forms an interpenetrating network through the particle interior. PIB is also present as a monolayer covering the particle surface. It is this surface layer of PIB that provides steric stabilization of these particles when dispersed in hydrocarbon media. A cartoon representation of this structure is presented in Figure 1.

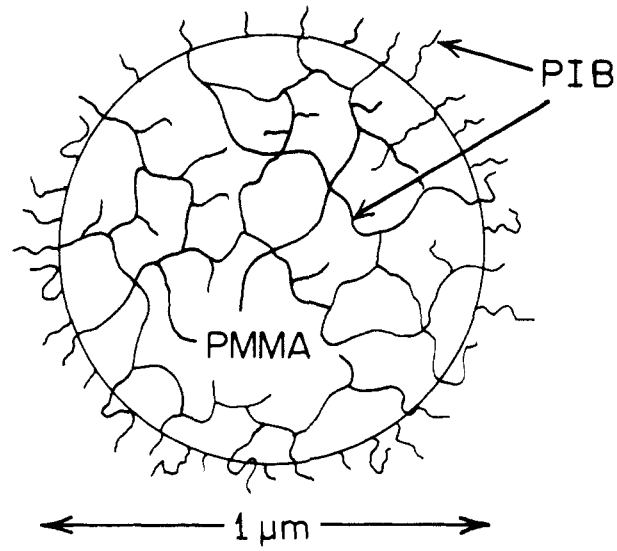

Figure 1. Cartoon representation of the interpenetrating network-type structure of the PMMA–PIB particles examined here.

Experimental Section

Anthracene- and phenanthrene-labeled PMMA–PIB polymer particles were prepared separately in a two-step process in which methyl methacrylate [MMA] in the first step was polymerized to low conversion in isooctane in the presence of PIB containing 2% isoprene units to promote grafting. The graft copolymer produced served as a dispersant in the second stage of polymerization, in which MMA was polymerized in an isooctane solution of the copolymer. Details have been reported elsewhere.[15,16] Stable spherical dispersions of polymer particles were produced, approximately 1 μm in diameter. A combination of ^{1}H NMR and UV analysis indicates that these particles contain 4 mol % monomer PIB and 0.052 mmol of An (An-labeled particles) and 0.0072 mmol of Phe groups (Phe-labeled particles) per gram of polymer, respectively. We refer to these particles as A and P.

Film preparations were carried out by two different methods. In the first, the same weights of A and P particles were dispersed in pentane in a 12-mm-o.d. quartz tube, and then pentane was removed by using a rotary evaporator. The particles formed a thin film on the inner surface of the quartz tube. Samples were outgassed by blowing nitrogen for 10 min. After sealing, tubes were placed into a temperature-controlled heating block. The thin film of particles was annealed above the glass transition temperature (T_g) of PMMA for various time periods and at different temperatures. In the second method, mechanical pressure was applied during film preparation. The same weights of A and P particles were mixed in the presence of pentane inside a centrifuge tube. After centrifugation, the pentane was removed and the dried mixture was placed in between Teflon sheets. Thin films were obtained using a Carver press under 5 tons of pressure, at various annealing temperatures and different time periods.

Fluorescence decay measurements were carried out by the time-correlated single photon counting technique employing a pulsed lamp source (Edinburg Instruments, 0.5 atm of D_2 gas) and a Hamamatsu 928 photomultiplier tube. Samples were excited at 295 nm and emission was detected at 345 nm. Data were collected over 3 decades of decay and fitted by nonlinear least squares using the δ-function convolution method[18] with BBOT (2,5-bis(5-*tert*-butyl-2-benzooxazolyl)thiophene) in ethanol as a standard. Data analysis allowed for a small correction due to scattered light[18] (the scatter parameter varied between 0.1 and 1.0). The uniqueness of the fit of the data to the model is determined by χ^2 ($\chi^2 \leq 1.5$), the distribution of the weighted residuals, and the autocorrelation of the residuals. All measurements were made at room temperature.

Fluorescence Decay Model for Coalescence

Direct nonradiative energy transfer is a Förster-type process between an electronically excited donor, D*, and an acceptor, A, whose rate, $W(r)$, varies with the separation r between D* and A and their mutual orientation:

$$W(r) = (3\kappa^2/2)(R_o/r)^6(1/\tau_D) \quad (1)$$

Here R_o is the critical Förster radius, which depends upon the spectroscopic properties of D and A, κ^2 is the orientational factor, and τ_D is the lifetime of excited donor. For a randomly oriented ensemble of immobile chromophores, $\kappa = 0.475$. Isolated donor molecules, which

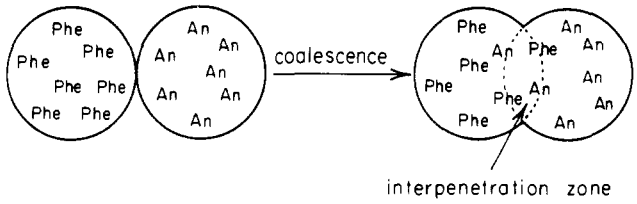

Figure 2. Representation of particle coalescence. Here the donor is phenanthrene (Phe) and the acceptor is anthracene (An).

do not undergo energy transfer, decay according to the expression

$$\phi_2(t) = B_2 \exp(-t/\tau_D) \quad (2)$$

Once coalescence begins, energy transfer can occur in the spatial domains where polymer molecules from adjacent particles mix. The survival probability of D* in these domains is described by the Förster equation

$$\phi_1(t) = B_1 \exp[-t/\tau_D - C(t/\tau_D)^{1/2}] \quad (3)$$

with

$$C = 4\pi^{3/2} N_A'[A] R_o^3 \quad (4)$$

Here [A] is the molar concentration of A in the domain and $N_A' = 6.023 \times 10^{20}$. For a representation of the coalescence process, see Figure 2.

When films are initially prepared, before any significant chain diffusion can occur, the measured fluorescence decay profile should be exponential. This statement presumes a negligibly small contribution to the fluorescence signal from energy transfer at the particle interface. Once coalescence begins and interparticle diffusion occurs, the fluorescence decay profile will have two contributions, a component (B_1) due to energy transfer

$$I(t) = B_1 \exp[-t/\tau_D - C(t/\tau_D)^{1/2}] + B_2 \exp(-t/\tau_D) \quad (5)$$

in the interpenetration domains and a component (B_2) due to D-labeled polymers that have not undergone mixing with A-labeled polymers (eq 5). If one mixes an equal number of otherwise identical particles, the ratio $B_1/(B_1 + 2B_2)$ gives the fraction[25] of donor- and acceptor-labeled polymers that have mixed, and the term C measures the concentration [A] in that region. Note the necessary but incorrect assumption that the acceptor concentration is uniform in the mixing region.

Results and Discussion

Energy Transfer. It is an absolute requirement for this type of experiment that the unquenched donor in the polymer film matrix exhibit a single-exponential decay. Such behavior is not common for organic dyes in glassy polymer matrices but is almost always found to be the case for 9-alkylphenanthrene derivatives. For this reason we chose D = Phe for these experiments. A typical fluorescence decay curve is presented in Figure 3 for a film of Phe-labeled particles. The decay is exponential, and on a longer time scale this decay remains exponential over 3 decades of the decay, with $\tau_D = 44$ ns.

We chose a 9-alkylanthracene derivative as the acceptor [A = An]. This particular pair of chromophores has an R_o value of 26 Å.[19] This value represents the distance at which a rotationally averaged ensemble of chromophore pairs would undergo energy transfer at the same rate as the unquenched decay rate [τ_D^{-1}] of the donor.

We prepared films by mixing an equal weight of Phe- and A-labeled PMMA particles, coating this on the inner wall of a 12-mm-o.d. quartz tube. The sample was deoxygenated with a stream of dry nitrogen gas, sealed with a rubber septum, and then heated above the glass transition temperature [T_g = 105 °C] of PMMA. Alternatively, we mixed an equal weight of Phe- and A-labeled particles, placed the mixture between Teflon sheets in a Carver press, and heated the mixture under pressure. In these latter experiments, the external pressure assists the deformation of the spherical particles, whereas in the case of particles coating the inner wall of the quartz tube, only surface tension effects and perhaps gravity contribute to particle shape deformation. These samples were allowed to cool to room temperature (22 °C) before fluorescence decay profiles were measured.

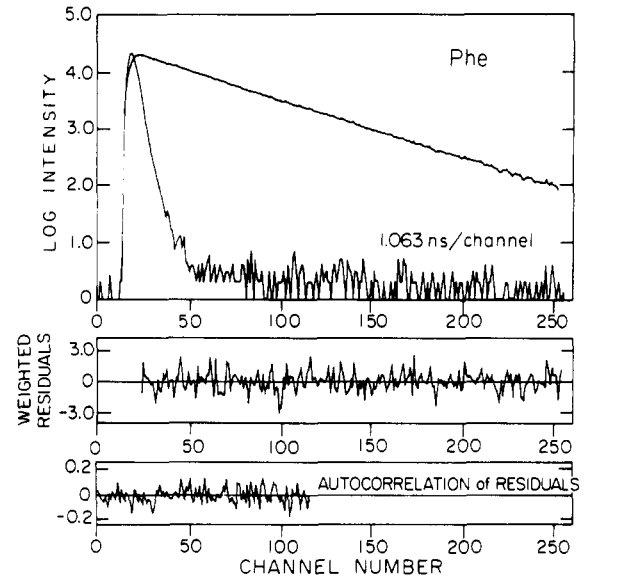

Figure 3. Monoexponential fluorescence decay of Phe in P particles, τ_0 = 44 ns.

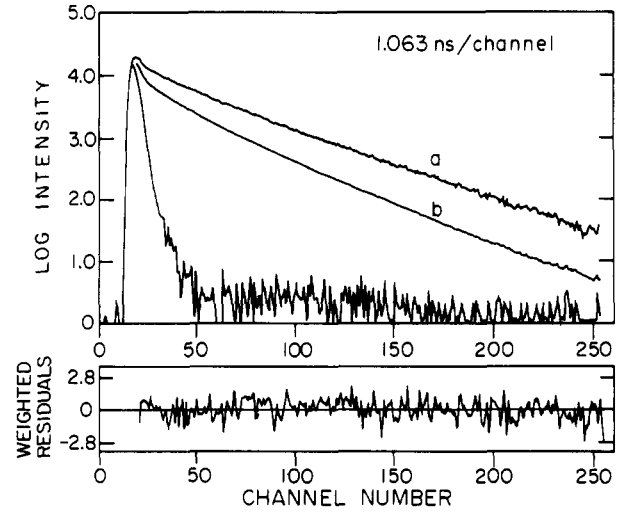

Figure 4. Fluorescence decay of Phe after annealing the film at 130 °C for 10 h under 5 tons of pressure: (a) solid line fit to eq 4, τ_0 = 44 ns (fixed), B_1 = 0.168, B_2 = 0.078, and C = 0.174, scatter parameter = 0.71 and χ^2 = 0.997; (b) Förster component of eq 4 for Phe decay.

In Figure 4 we present a fluorescence decay trace obtained from a film pressed at 130 °C for 1 h at 5 tons of pressure in the Carver press. One notes a strong deviation from exponential decay. The curve can be fitted to eq 5 to obtain the parameters shown in the caption to Figure 4. In this fit, τ_D is set at the value determined independently. In the lower curve in Figure 4, we present a simulated decay curve for the Förster DET component of this decay. The differences between the two decay

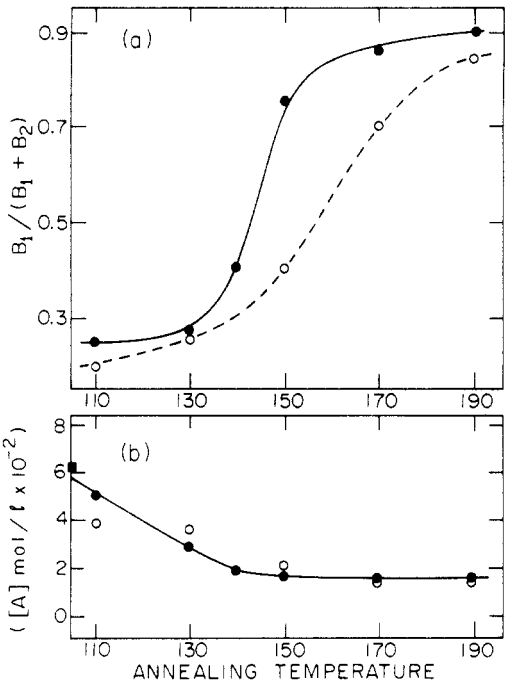

Figure 5. (a) $B_1/(B_1 + B_2)$ ratios of films annealed 1 h at each temperature. (b) Variation of anthracene concentration [A], with annealing temperature. [A] values were obtained from eq 3. Open circles refer to experiments with no external pressure, and closed circles, to samples heated under 5 tons of external pressure.

curves are due to the contribution of the B_2 term in eq 5 to the observed decay profile.

In this way fluorescence decay profiles from a variety of samples were analyzed, and values of B_1, B_2, and C were obtained. Values of $B_1/(B_1 + B_2)$ vs annealing temperature are plotted in Figure 5 for a series of samples heated for 1 h at each of the temperatures indicated. Under the two sets of conditions (with and without external pressure) this ratio does not achieve its saturation value of unity. This point was checked by dissolving a mixture of Phe- and A-labeled particles in a solvent (ethyl acetate) and casting a film. Under these circumstances the ratio $B_1/(B_1 + B_2)$ had a value of 0.96. The fact that this ratio is somewhat less than unity may be due to complexities in coalescence caused by the 4 mol % PIB present in the system.

Interparticle polymer diffusion also leads, as it should, to a decrease in the local concentration [A]. These values can be calculated from the measured parameter C and eq 4 and are shown in the lower portion of Figure 5. The initial value of [A] (0.052 mmol of A/g of PMMA; 6.2×10^{-2} M) is known from the composition of the An-labeled particles. This point is shown as the square in Figure 5. Only after some chain interpenetration has occurred can an experimental value of [A] be obtained. These "initial" values of [A] are somewhat smaller and decrease with increasing time or temperature to 2×10^{-2} M. This decrease is larger than the 2-fold dilution expected on the basis of our model and represents a point to be investigated in future experiments.

We present another look at the coalescence process in Figure 6. Here we compare the extent of chain mixing as a function of time for samples heated to 130 °C. It is clear that the effect of external pressure is significant, especially at this temperature, only 22 °C above T_g for PMMA. The role of external pressure here is most likely to drive particle deformation, to produce void-free films, and to maximize the interparticle contact area.

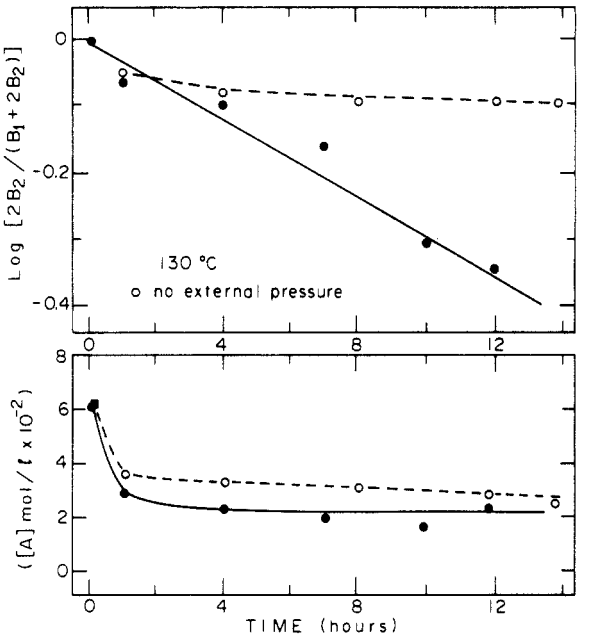

Figure 6. (a) Plots of log $[2B_2/(B_1 + 2B_2)]$ vs t at a 130 °C annealing temperature. (b) Variation of [A] with time at a 130 °C annealing temperature. Open circles, no external pressure; closed circles, 5 tons of external pressure.

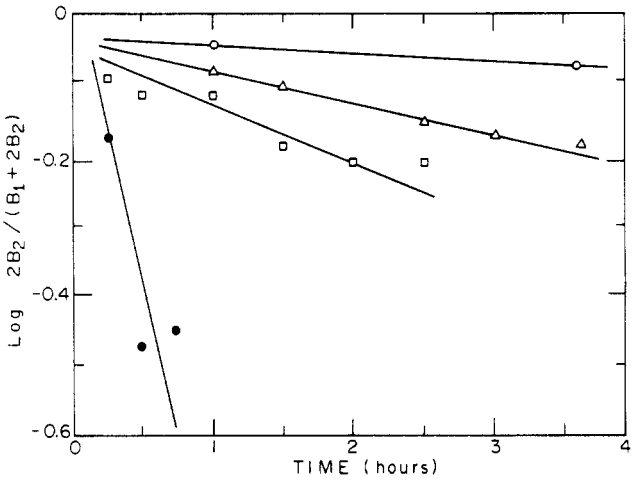

Figure 7. Plots of log $[2B_2/(B_1 + 2B_2)]$ vs t at different annealing temperatures for samples heated with no external pressure: (○) 130 °C; (△) 150 °C; (□) 160 °C; (●) 170 °C.

Polymer Diffusion. The results described above demonstrate that polymer diffusion across the particle boundary takes place. To obtain quantitative information, we must fit this data to a model describing the diffusion. Several models are possible, and the problem is made more delicate by the expected molecular weight dependence of the polymer self-diffusion coefficient, coupled with the large molecular weight polydispersity in the samples. This problem is common to all studies of latex film formation, and it is clear that, in the long term, one will have to pay considerable attention to the issue of which model and what type of data analysis best describe the physics of the coalescence process.

In latex film formation, particle deformation to close-packed polyhedra precedes coalescence. As a consequence, we have chosen here a planar sheet model for Fickian diffusion of polymer chains across the particle interface. Such diffusion is described by the equation[20]

$$\frac{M_t}{M_\infty} = 1 - \frac{8}{\pi^2}\sum_{n=0}\frac{1}{(2n+1)^2}\exp\left[-\frac{D(2n+1)^2\pi^2 t}{a^2}\right] \quad (6)$$

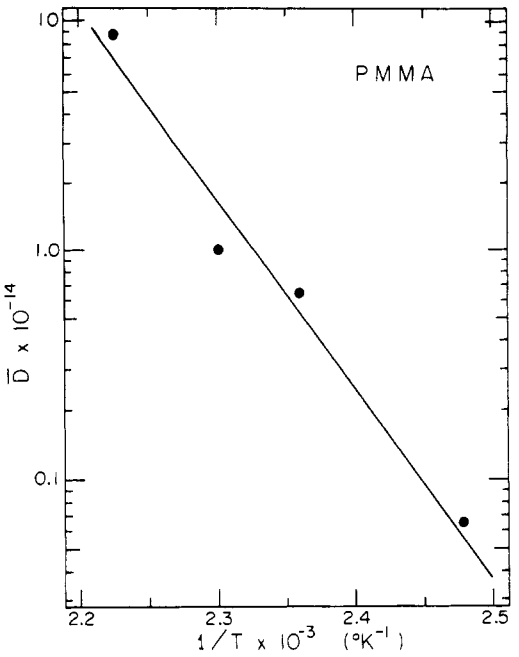

Figure 8. Arrhenius plot of $\bar{D}$ values obtained from film samples heated with no external pressure.

where M_t is the amount of substance that has diffused across the interface at time t and a is the maximum distance over which diffusion can occur. M_∞ is the value of M_t at $t = \infty$. In these experiments we consider only the first term in the summation on the right-hand side of eq 6 and let a equal the radius of the particle undergoing coalescence.

$$\left[1 - \frac{B_1}{B_1 + 2B_2}\right] = \left[1 - \frac{M_t}{M_\infty}\right] \approx \exp(-\pi^2 Dt/a^2) \quad (7)$$

Plots of $\log [2B_2/(B_1 + 2B_2]$ vs t are presented in Figure 7 for films formed in the absence of external pressure. The plots are linear for each of the temperatures, as predicted by eq 7, and from the slopes, values for D can be calculated. These are very sensitive to temperature and range from 6×10^{-16} cm^2 s^{-1} at 130 °C to 8.9×10^{-14} cm^2 s^{-1} at 170 °C. These values are in the same range as those found by Hahn et al. using neutron scattering to follow poly(butyl methacrylate) latex fusion at 60 °C above T_g. In addition, our D values give a linear Arrhenius plot with an apparent activation energy of 37 kcal/mol (corr = 0.983).

For simple homopolymer systems, theory[21] predicts that the ratio of D/T will show the same temperature dependence as the inverse zero-shear viscosity, η^{-1}. This prediction follows from the idea that the temperature dependence of both phenomena is dominated by that of the monomeric friction coefficient. Both diffusion and zero-shear viscosity data should be described by the WLF equation.[22] For diffusion, this equation is written as

$$\log \frac{DT_0}{D_0 T} = \frac{(C_1^0 T - T_0)}{C_2^0 + T - T_0} \quad (8)$$

where D_0 represents the diffusion coefficient at the reference temperature T_0 and C_1^0 and C_2^0 are parameters obtained from analysis of shear viscosity measurements relative to the chosen T_0. This type of behavior is well-documented for self-diffusion of polymers in melts.[23]

A disturbing feature of the results reported here is that the temperature dependence of D is much smaller than that calculated from eq 8 using C_1^0 and C_2^0 values appropriate to PMMA.[22] This difference can be emphasized in another way. Ferry[22] has shown that the apparent activation enthalpy, ΔH_a(app), obtained from an Arrhenius plot of D or η^{-1} can be calculated from the expression

$$\Delta H_a(\text{app}) = \frac{2.303RC_1^0 C_2^0 T^2}{(C_2^0 + T - T_0)^2} \quad (9)$$

where R is the gas constant. Note that ΔH_a(app) depends upon temperature. From eq 9 and C_1^0 and C_2^0 values appropriate to PMMA, we calculate ΔH_a(app) = 192 kcal/mol at 403 K and 114 kcal/mol at 449 K, the range of temperatures over which we determined D by energy transfer. These values are significantly higher than that (37 kcal/mol) found in Figure 8.

We do not understand the origin of these differences, although the apparent activation energy we find does correspond to that of backbone motion of PMMA.[24] The model we use to obtain D values from energy-transfer data may be one source of problems, and the molecular weight polydispersity may be another. These are points that will require close scrutiny in future experiments.

Summary

We report the first experiments which use energy-transfer measurements to follow polymer diffusion across the particle boundary during latex film formation. These follow the fraction of mixing of time and provide data from which we calculate the mean diffusion coefficient characterizing polymer diffusion in the system. For PMMA particles at temperatures between 403 and 450 K, D takes values ranging from 6×10^{-16} to 9×10^{-14} cm^2 s^{-1}.

Acknowledgment. We thank NSERC, Canada, for its generous financial support of this research, as well as the Province of Ontario through its URIF program.

References and Notes

(1) Fluorescence Studies of Polymer Colloids. 25.
(2) Permanent address: Department of Physics, Istanbul Technical University, Istanbul, Turkey.
(3) Morgan, L. W. *J. Appl. Polym. Sci.* **1982**, *27*, 2033.
(4) Myers, R. R.; Shulz, R. K. *J. Appl. Polym. Sci.* **1964**, *8*, 755.
(5) Kast, H. Aspects of Film Formation with Emulsion Copolymers. *Makromol. Chem. Suppl.* **1975**, *10/11*, 447–461.
(6) Eckersley, S. T.; Rudin, A. *J. Coatings Technol.* **1990**, 62.
(7) Distler, D.; Kanig, G. *Colloid Polym. Sci.* **1978**, *256*, 1052.
(8) Vanderhoff, J. W.; Bradford, E. B.; Carrington, W. K. *J. Polym. Sci., Polym. Symp.* **1973**, *41*, 155.
(9) Chainey, M.; Wilkinson, M. C.; Hearn, J. *J. Polym. Sci. Polym. Chem. Ed.* **1985**, *23*, 2947.
(10) (a) Hahn, K.; Ley, G.; Schuller, H.; Oberthur, R. *Colloid Polym. Sci.* **1986**, *264*, 1092. (b) Hahn, K.; Ley, G.; Oberthur, R. *Colloid Polym. Sci.* **1988**, *264*, 631.
(11) (a) Linne, M. A.; Klein, A.; Miller, G. A.; Sperling, L. H.; Wignall, G. D. *J. Macromol. Sci., Phys.*, **1988**, *B27*, 217. (b) Linne, M. A.; Klein, A.; Sperling, L. H.; Wignall, G. D. *J. Macromol. Sci., Phys.* **1988**, *B27*, 181.
(12) Förster, T. *Discuss. Faraday Soc.* **1959**, *27*, 7.
(13) (a) Morawetz, H. *Science* **1988**, *240*, 172. (b) Mikes, F.; Morawetz, H.; Dennis, K. S. *Macromolecules* **1980**, *13*, 969.
(14) Napper, D. *Polymeric Stabilization of Colloidal Dispersion*, Academic Press; London, 1983.
(15) Peckan, Ö.; Winnik, M. A.; Croucher, M. D. *J. Colloid Interface Sci.* **1983**, *95*, 420.
(16) Winnik, M. A.; Pekcan, Ö.; Chen, L.; Croucher, M. D. *Macromolecules* **1988**, *21*, 55.
(17) Pekcan, Ö.; Winnik, M. A.; Croucher, M. D. *Phys. Rev. Lett.* **1988**, *61*, 641.
(18) Martinho, J. M. G.; Egan, L. S.; Winnik, M. A. *Anal. Chem.* **1987**, *59*, 861.
(19) Berlman, I. B. *Energy Transfer Parameters of Aromatic Compounds*; Academic Press: New York, 1973.

(20) Crank, J. *Mathematics of Diffusion*, 2nd ed.; Clarendon Press; Oxford, 1975.
(21) Doi, M.; Edwards, S. F. *The Theory of Polymer Dynamics*; Oxford University Press: Oxford, 1986.
(22) Ferry, J. D. *Viscoelastic Properties of Polymers*, 3rd ed.; Wiley: New York, 1980; Chapter 11.
(23) See for example: (a) Mumbry, S. J.; Smith, B. A.; Samulski, E. T.; Yu, L.-P.; Winnik, M. A. *Polymer* **1986**, *27*, 1826. Green, P. F.; Russell, T. P.; Jerome, R.; Granville, M. *Macromolecules* **1989**, *22*, 908.
(24) Johnson, F.; Padon, J. C. *J. Polym. Sci., Polym. Chem. Ed.* **1973**, *11*, 1995.
(25) Note Added in Proof: We now appreciate that $B_1/(B_1 + 2B_2)$ measures the *number fraction* of donors in the interpenetration zone. If one assumes a uniform acceptor concentration in this domain and accounts for the dilution of acceptors upon mixing, the *volume fraction* of mixing is equal to $B_1/(B_1 + B_2)$. This topic is discussed in more detail in: Zhao, C.-L.; Wang, Y.; Hruska, Z.; Winnik, M. A.; Croucher, M. D. *Macromolecules*, in press.

Registry No. (MMA)(IB)(isoprene) (graft copolymer), 116945-20-1.

Main-Chain Reorientation in Polycarbonates

Mark D. Poliks, Terry Gullion, and Jacob Schaefer*

Department of Chemistry, Washington University, St. Louis, Missouri 63130

Received June 22, 1989; Revised Manuscript Received November 28, 1989

ABSTRACT: The amplitudes of main-chain reorientations have been determined by dipolar rotational spin-echo ^{13}C NMR for bisphenol A polycarbonate, for the phenoxy resin made from bisphenol A and formaldehyde, and for the phenoxy resin made from bisphenol A and epichlorohydrin. All three polymers display prominent low-temperature mechanical-loss peaks, and all three polymers have main-chain rings undergoing rapid 180° flips at room temperature. The present results show that the amplitude of the main-chain rotational reorientation at the isopropylidene position for bisphenol A polycarbonate, and the isopropylidene and carbonate positions for the other two polymers, is less than 20° (root-mean-square). Small-amplitude motion at the carbonate position in bisphenol A polycarbonate has been observed before in measurements of carbonyl carbon chemical-shift tensors. Similar small-amplitude motion at the carbonate position has also been inferred from measurements of the volumes of activation for the ring-flip processes in bisphenol A polycarbonate and the phenoxy resin made from bisphenol A and epichlorohydrin. The combination of all of these results leads to the conclusion that the same kind of small-amplitude lattice reorganization controls ring flips for all three of these polycarbonates.

Introduction

The hydrostatic pressure dependence of the ring-flip process in polycarbonate (PC) and in the phenoxy resin made from bisphenol A and epichlorohydrin (PK) has been discussed recently in terms of the densification of chain packing in the glassy state.[1] In this description, steric interactions between *several* chains in the lattice are assumed ultimately to control the ring flips. This model of the ring-flip process in polycarbonates differs significantly from the defect-diffusion model proposed by Jones.[2] In the defect-diffusion model, the dominant physics is contained in the rotational reorientation of conformational defects within a *single* chain. Defects are assumed to diffuse up and down the long axis of the chain, with rings flipping as defects pass. Variations in the rate of defect diffusion result from variations in the local mean-field viscosity of the lattice. The defect-diffusion model has been used to interpret both NMR line shapes[3] and the results of mechanical loss experiments[4] and also has been invoked as a possible explanation for polycarbonate's aging, and its viscoelastic, and thermodynamic behavior.[5]

In this paper we report the results of ^1H–^{13}C dipolar rotational spin-echo experiments on PC, on PK, and on the phenoxy resin formed from bisphenol A and formaldehyde (FPC). These polymers differ in the carbonate, or carbonate-like, main-chain linkages connecting aromatic moieties. The carbonate linkages for the three polymers are as follows: PC, $-OC(=O)O-$; PK, $-OCH_2CH(-OH)CH_2O-$; and FPC, $-OCH_2O-$. Despite differences in the carbonate linkages, all three polymers display similar low-temperature mechanical-loss peaks[1] and all three polymers have rings undergoing rapid 180° flips at room temperature. The present NMR experiments are designed to measure the amplitudes of main-chain motions of the isopropylidene units in PC and PK and the carbonate-like units in FPC and PK. The results of these experiments indicate only small-amplitude main-chain motion at both isopropylidene and carbonate sites.

Experimental Section

Magic-Angle Spinning. Cross-polarization magic-angle spinning ^{13}C NMR spectra were obtained at room temperature on a spectrometer built around a 12-in. iron magnet operating at a proton Larmor frequency of 60 MHz.[6] Half-gram samples were spun in a double-bearing rotor[7] at 1859 or 930 Hz. The long-term stability of the spinning speed was ±1 Hz.

Carbon Dipolar Sideband Patterns. Carbon dipolar line shapes were characterized by dipolar rotational spin-echo (DRSE) ^{13}C NMR at 15.1 MHz. This is a two-dimensional experiment[8] in which, during the additional time dimension, carbon magnetization is allowed to evolve under the influence of H–C coupling while H–H coupling is suppressed by homonuclear multiple-pulse semiwindowless MREV-8 decoupling.[9] The cycle time for the homonuclear decoupling pulse sequence was 33.6 μs, resulting in decoupling of proton–proton interactions as large as 60 kHz. Sixteen MREV-8 cycles fit exactly in one rotor period so that strong dipolar echoes formed. A 16-point Fourier trans-

0024-9297/90/2223-2678$02.50/0